JOURNAL OF MATERIALS SCIENCE 11 (1976) 1278–1287

Reaction sintered silicon nitride

Part 1 *The influence of oxygen and water vapour contamination on strength and composition*

D. P. ELIAS, M. W. LINDLEY
Procurement Executive, Ministry of Defence, Admiralty Materials Laboratory, Poole, Dorset, UK

The strength, composition and structure of reaction sintered silicon nitride formed in the presence of oxygen or water vapour have been investigated. It is shown that chemical contamination of the nitriding gas by oxygen and water vapour to relatively high concentrations is not the cause of abnormally low strength silicon nitride. The coefficient of variation in strength and "apparent" crystallite size for a particular batch of samples are related to the water vapour concentration in the nitriding gas. The formation of α- and β-silicon nitride is discussed and it is suggested that compositional variations in α-silicon nitride must be small.

1. Introduction

Reaction sintered silicon nitride (or reaction bonded silicon nitride) may be used in high temperature engineering applications such as diesel engines and gas turbines [1] if it can be fabricated to reproducible high strengths with a low strength variability. We have found [2, 3] as have other workers that this is difficult to achieve, and frequently lower than normal and occasionally abnormally low strengths are recorded [4]. Reaction sintered silicon nitride is formed by complex reactions involving not only silicon, nitrogen and silicon monoxide, but also solid impurities such as iron, calcium and iron compounds, and gaseous impurities such as oxygen and water vapour. Although the influence of solid impurities is important, gas phase impurities may also be important since large variations in composition and mechanical properties have been reported for silicon nitride prepared from the same silicon powder in consecutive experiments in the same furnace [4].

The influence of low concentrations* ($\sim 10^{-6}$ to 10^{-4}) of gas phase impurities on the kinetics of the nitriding reaction (e.g. [5–7]) and the products of nitridation (e.g. [8–12]) have been studied extensively but the influence on strength is not clear. Abnormally low strengths have been tentatively ascribed to contamination of the nitriding gas (e.g. leaks in the furnace or gas lines), but preliminary data on the influence of water vapour contamination do not support this [4]. It is important, therefore, to establish the precise role and effect of gaseous contaminants and this paper is specifically concerned with oxygen and water vapour and their influence on the strength and structure of reaction sintered silicon nitride: the data may further clarify the complex role of oxygen in the formation of α-silicon nitride [13–19].

2. Experimental

The silicon powder had a median particle size of 25 μm and a maximum particle size of 75 μm. The major cation impurities were (wt%) Fe 0.65, Al 0.28, Ca 0.27, Ti 0.06, other impurities < 0.01, and the oxygen content was 0.5. The preparation of test bars from argon sintered silicon compacts has been described elsewhere [2]. In each experiment bars were nitrided for 2 h at 1250° C, 50 h at 1350° C and 10 h at 1450° C in a vacuum-tight mullite furnace tube; the bars were weighed and measured before and after each experiment. In the majority of experiments ("static" experiments) the gas pressure was maintained at 7 kN m^{-2} above

* All gas concentrations are expressed as volumes per unit volume.

atmospheric, gas entry into the furnace being controlled by the rate of reaction of the silicon compacts with the furnace atmosphere. In other experiments ("flow" experiments) there was a continuous gas flow ($\sim 100\,ml\,min^{-1}$) through the furnace tube whilst the compacts were being nitrided. The bars were nitrided in three experimental series: series A – "static" experiments: water vapour added to nitrogen; series B – "static" experiments: oxygen added to nitrogen; series C – "flow" experiments: oxygen added to nitrogen.

Series A experiments are not strictly comparable with series B and C experiments because a different furnace was used for the latter experiments although this furnace was of the same design and construction as the furnace used for series A experiments. Series A experiments were performed at a constant oxygen concentration of 5×10^{-6} and water vapour concentrations in the range 3.5×10^{-5} to 6×10^{-3} as measured by an electrolytic hygrometer. The water vapour concentrations in series B and C experiments were approximately 3.5×10^{-5} and oxygen concentrations were varied in the range 5×10^{-6} to 2×10^{-1} (1×10^{-1} maximum for series C). In series C experiments, a continuous recording of the oxygen potential of the gas leaving the furnace was obtained using a stabilized zirconia oxygen meter operating at 800° C.

Fracture strengths were determined for all bars at room temperature using as-nitrided surfaces tested in three-point bend with a span of 19.05 mm: some tests were also conducted at 1350° C in air. One fractured bar from each experiment was selected for analysis for its oxygen content (by neutron activation analysis), phase content and unit cell dimensions (for α- and β-silicon nitrides): the weight gain of this bar was typical of its batch. At high gas impurity concentrations in flow experiments large variations in sample weight gain and strength were observed; the samples showing these variations were also analysed. The crystalline phases were determined by X-ray diffractometry. The specimens were either polished centre sections from the strength bars cut lengthwise, or, where preferred orientation effects were observed for silicon reflections, the samples were ground to pass a 200 BS sieve before X-ray analysis. The weight ratios of the phases were estimated from standardization curves [20, 21] using the following pairs of reflections: β-Si_3N_4 (1 0 1) and α-Si_3N_4 (1 0 2); β-Si_3N_4 (2 1 0) and α-Si_3N_4 (2 1 0); Si (2 2 0) and α-Si_3N_4 (2 1 0); Si (1 1 1) and α-Si_3N_4 (2 0 1): the accuracy is estimated to be better than ± 2%. The unit cell dimensions were calculated from high Bragg angle reflections using the "Firestar" computer program [22].

3. Results

Crystalline phases, strengths and sample oxygen contents are shown in Tables I to III. These data were obtained from silicon nitride test bars of density 2.55 to 2.60 $Mg\,m^{-3}$ prepared from silicon compacts of density circa 1.58 $Mg\,m^{-3}$.

3.1. Crystalline phases

The amount of α-silicon nitride formed in series A experiments (Table I) was invariant with concentrations of water vapour up to 3.5×10^{-3}, and increased to 90% at a water vapour concentration of 6×10^{-3}. For both series B and C experiments (Tables II and III and Fig. 1) the amount of α-silicon nitride reached a maximum at an oxygen concentration of 1×10^{-2} with a corresponding minimum in the amount of β-silicon nitride: for series B there were significantly higher α- and lower β-silicon nitride contents than for series C.

At high oxygen concentrations, the phases

TABLE I Strength and compositional data for water vapour additions to the nitriding gas – "static" experiments (series A)

Expt.	Water vapour concn.	Compact weight gain (%)	Crystalline phases (%)			Line width $Bw \times 10^3$ rad		Sample oxygen (wt %)	Batch strength		
			α-Si_3N_4	β-Si_3N_4	Si	α_{540}	β_{323}		Mean ($MN\,m^{-2}$)	No. bars	Coeff. var (%)
1	3.5×10^{-5}	63.5	80	19	1	6.6	9.3	0.71	247 ± 10	7	4.0
2	1.4×10^{-4}	61.8	81	19	<1	6.1	7.7	0.60	231 ± 7	6	2.9
3	6.0×10^{-4}	61.5	80	19	1	5.6	8.5	0.53	233 ± 6	5	2.8
4	3.5×10^{-3}	64.0	80	20	<1	4.9	7.0	0.87	229 ± 5	6	2.0
5	4.4×10^{-3}	64.0	87	13	<1	6.3	8.7	0.53	246 ± 12	18	4.8
6	6.0×10^{-3}	64.1	90	10	<1	7.3	9.4	0.54	234 ± 14	19	5.9

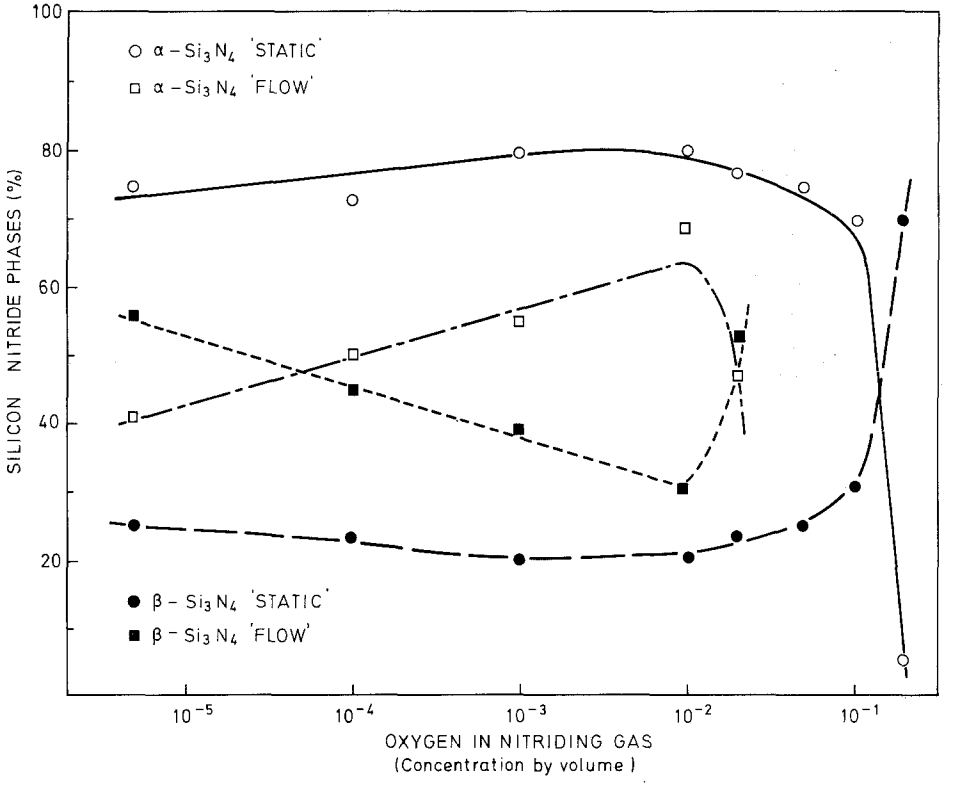

Figure 1 The amount of α- and β-silicon nitride phases versus oxygen concentration in the nitriding gas for "static" and "flow" experiments.

formed depended not only upon the oxygen concentration, but also upon the position of the specimen within the furnace. This is exemplified in series C for an oxygen concentration of 5×10^{-2}, when the principal phases were cristobalite in a specimen nearest the gas inlet, and silicon oxynitride in a specimen near the centre of the hot zone of the furnace.

For series C, the measured oxygen concentrations of the exhaust gases (in the zirconia meter at 800° C) during nitriding at 1350° C were $\sim 10^{-19}$ (inlet concn. 5×10^{-6}) to 10^{-17} (inlet concn. 1×10^{-2}) and in this range only α- and β-silicon nitride and silicon phases were observed. At higher inlet concentrations the oxygen content of the inlet and exhaust gases were similar and under these conditions silicon oxynitride and cristobalite were formed.

TABLE II Strength and compositional data for oxygen additions to the nitriding gas – "static" experiments (series B)

Oxygen concn.	Compact weight gain (%)	Crystalline phases (%)				Sample oxygen (wt %)	Batch strength	
		α-Si_3N_4	β-Si_3N_4	Si	Si_2N_2O		Mean (MN m^{-2})	No. bars
5×10^{-6}	63.2	75	25	<1	nd	nm	219 ± 15	12
1×10^{-4}	62.5	73	23	4	nd	1.00	195 ± 19	12
1×10^{-3}	62.5	80	20	<1	nd	0.48	221 ± 12	14
1×10^{-2}	62.1	80	20	<1	nd	0.48	220 ± 9	12
2×10^{-2}	61.7	77	23	<1	nd	0.70	244 ± 13	12
5×10^{-2}	60.6	75	25	<1	nd	0.63	204 ± 10	13
1×10^{-1}	62.3	69	31	<1	nd	0.88	213 ± 18	12
2×10^{-1}	56.0	5	70	5	20	4.13	90 ± 15	12

nd – not detected
nm – not measured

TABLE III Strength and compositional data for oxygen additions to the nitriding gas – "flow" experiments (series C)

Oxygen concn.	Compact weight gain (%)	Crystalline phases (%)					Sample oxygen (wt %)	Batch strength	
		α-Si_3N_4	β-Si_3N_4	Si	Si_2N_2O	SiO_2		Mean ($MN\,m^{-2}$)	No. bars
5×10^{-6}	62.1	41	56	3	nd	nd	nm	168 ± 8	10
1×10^{-4}	61.0	50	46	4	nd	nd	0.43	182 ± 15	10
1×10^{-3}	58.1	55	40	5	nd	nd	0.47	144 ± 17	12
1×10^{-2}	60.9	69	31	<1	nd	nd	0.84	154 ± 21	12
2×10^{-2}	61.4	47	53	<1	nd	nd	0.78	167 ± 17	14
5×10^{-2}	16.2	nd	nd	57	43	nd	10.8	30 ± 10	14
5×10^{-2}	39.9*	nd	nd	90	nd	10	27.8	30 ± 10	14
1×10^{-1}	40.0	nd	nd	90	nd	10	29.1	27 ± 3	12

nd – not detected
nm – not measured
* Sample exhibiting "extreme" properties (Section 3.1).

TABLE IV Summary of unit cell dimensions for α-silicon nitrides

	a (Å)	c (Å)
Prepared by nitridation of silicon		
Present work	7.749–7.754	5.618–5.621
[13, 28–34]	7.747–7.758	5.616–5.623
Prepared from silicon compounds		
[15, 17, 19, 35, 36]	7.752–7.818	5.591–5.625

3.2. Unit cell dimensions

The unit cell dimensions for α-silicon nitride are summarized in Table IV, together with data published previously for this phase. The range of values for the cell dimensions of β-silicon nitride were $[a] = 7.593 \pm 0.004$ to 7.602 ± 0.002 Å and $[c] = 2.906 \pm 0.001$ to 2.908 ± 0.001 Å. There was no significant trends between cell dimensions and oxygen or water vapour concentrations, or the measured oxygen contents of the samples.

3.3. X-ray profile shapes

Systematic changes in X-ray profile shapes with water vapour concentration were observed for high 2θ reflections: these effects were not observed in series B or C. The $K\alpha_1$ profile shapes of the α_{540} and β_{323} peaks and their background regions were determined by automatic step scanning. The peak widths (Bw) at half peak height are shown in Table

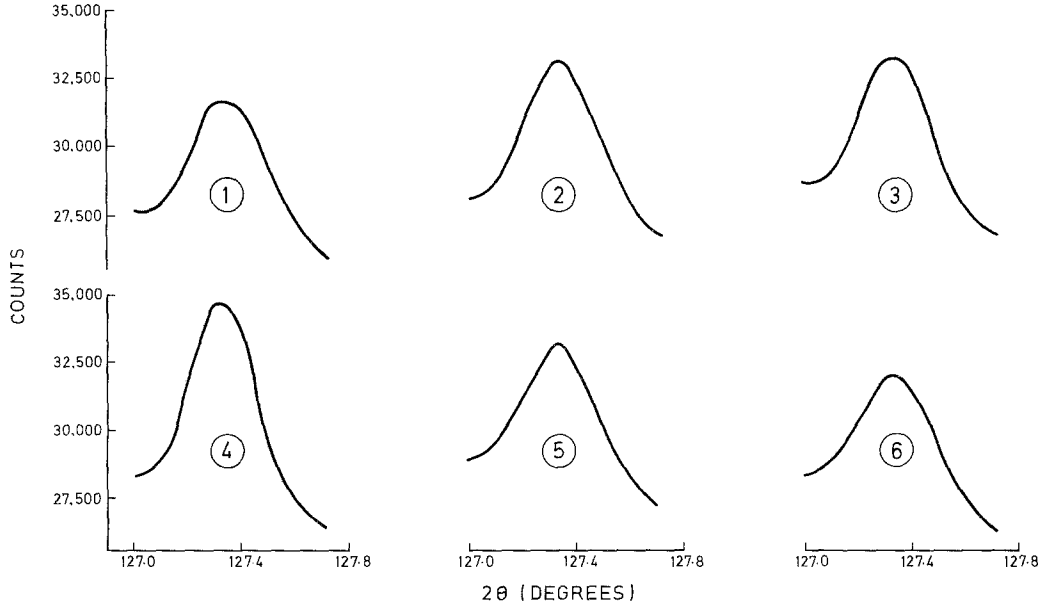

Figure 2 α-silicon nitride (5 4 0) peaks for differing water vapour concentrations in the nitriding gas. (1–6 refer to the experiment numbers in Table I.)

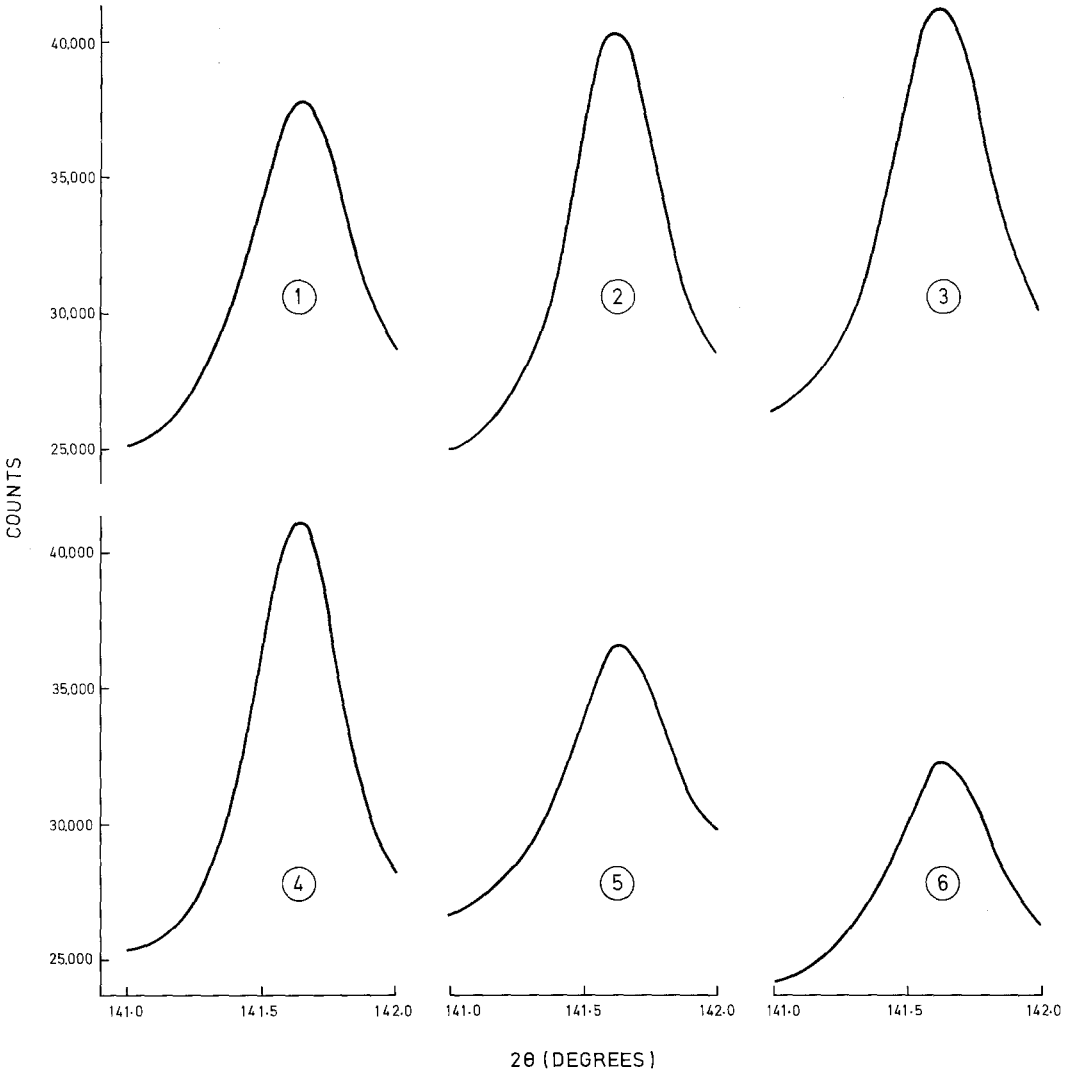

Figure 3 β-silicon nitride (3 2 3) peaks for differing water vapour concentrations in the nitriding gas. (1–6 refer to the experiment numbers in Table I.)

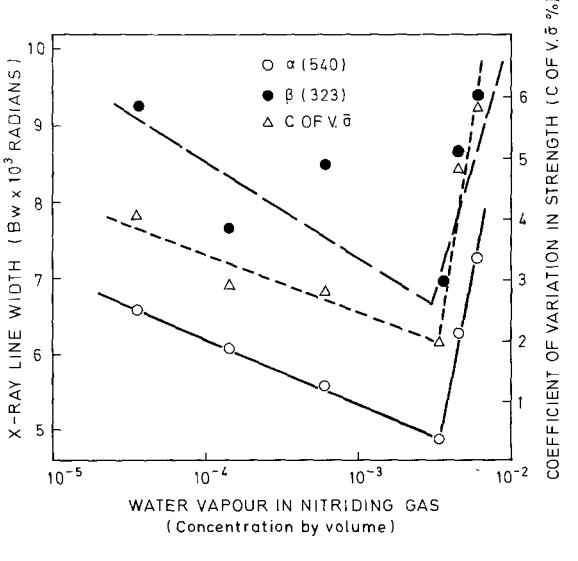

Figure 4 X-ray line widths *Bw* and coefficient of variation in strength versus water vapour concentration of the nitriding gas.

I and the central regions of the peaks in Figs. 2 and 3. Fig. 4 shows a well defined trend between water vapour concentrations and the X-ray peak widths for the α_{540} and β_{323} reflections and the coefficient of variation in strength. Minima in *Bw* and the coefficient of variation in strength occur at a water vapour concentration $\sim 3.5 \times 10^{-3}$.

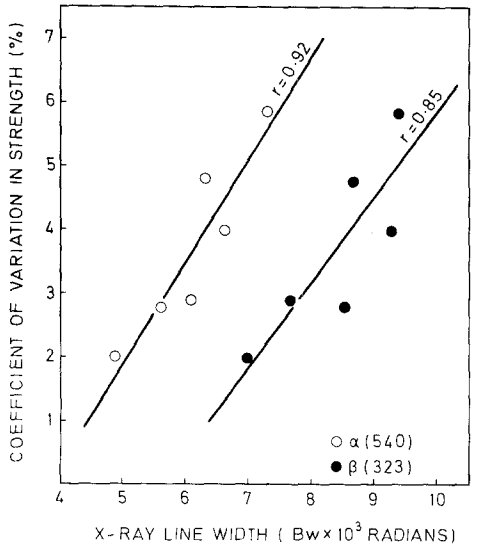

Figure 5 Coefficient of variation in strength versus X-ray line widths *Bw* for the α-nitride (5 4 0) peaks and β-nitride (3 2 3) peaks. The straight lines are the least squares fit and *r* is the correlation coefficient.

There are separate linear relationships (Fig. 5) between *Bw* and the coefficient of variation in strength for α_{540} reflections (correlation of data $r = 0.92$) and β_{323} reflections ($r = 0.85$): these relationships are independent of water vapour concentration for the range considered in this work.

3.4. Strength

For series A the mean room temperature strengths were invariant with water vapour concentration. For series B and C, mean strengths were invariant with oxygen to concentrations of 1×10^{-1} and 2×10^{-2} respectively: at higher oxygen concentrations marked reductions in strength were observed (Fig. 6) but these were associated with significant changes in the crystalline phases formed (Tables II and III). The mean strengths for "flow" experiments (series C) were significantly lower than the mean strengths for "static" experiments (series B). The strengths at 1350° C of samples prepared in "static" experiments at oxygen concentrations of 2×10^{-2} and 5×10^{-2} were 224 ± 17 and $144 \pm 18\,MN\,m^{-2}$ respectively.

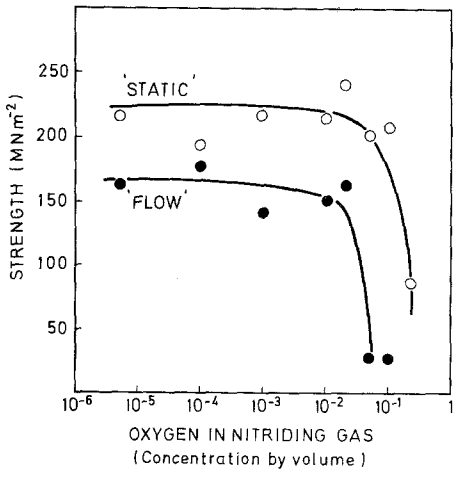

Figure 6 Room temperature strength versus concentration of oxygen in the nitriding gas for "static" and "flow" experiments.

4. Discussion

4.1. Room temperature strength

Room temperature strengths for "static" experiments for all water vapour concentrations, and oxygen concentrations to 1×10^{-1} are similar to data from samples prepared with normal nitriding atmospheres [2] and confirm earlier data on the invariance of mean strength with water vapour to concentrations of 3.5×10^{-3} [4]. These data show that contamination of the nitriding gas to these concentrations by water vapour or oxygen does not result in the formation of abnormally low strength silicon nitride.

The room temperature strengths (to oxygen concentrations of 2×10^{-2}) of nearly completely nitrided samples are significantly lower in "flow" experiments than "static" experiments. These observations form the subject of the succeeding paper in this journal [23].

4.2. High temperature strength

Subtle differences may exist, however, between samples prepared at relatively high oxygen concentrations in "static" experiments. The bend strengths of samples prepared at an oxygen concentration of 2×10^{-2} were not significantly different at room temperature and 1350° C (244 ± 13 and $244 \pm 17\,MN\,m^{-2}$ respectively) and consistent with other high temperature strength data for normal reaction sintered silicon nitride [24]. At an oxygen concentration of 5×10^{-2}, however, the mean strength at 1350° C ($144 \pm 18\,MN\,m^{-2}$) was some 30% lower than the room

temperature value. These differences in high temperature strength may be due to the type, and distribution rather than amount of any amorphous phases since the crystalline phases and oxygen contents were not significantly different for samples prepared at oxygen concentrations of 2×10^{-2} and 5×10^{-2}.

4.3. The formation of α- and β-silicon nitride

Increasing the concentration of water vapour and of oxygen (up to 1×10^{-2}) in the nitriding gas results in the formation of increasing amounts of α-silicon nitride (Tables I to III and Fig. 1). These results may be explained if it is postulated that α-silicon nitride forms by a reaction involving silicon monoxide and nitrogen (e.g. [25]) whereas β-silicon nitride forms by a direct reaction involving silicon and nitrogen. Evidence in favour of the formation of β-silicon nitride from silicon vapour is discussed in Section 4.5.

At nitriding temperatures, silica formed from the action of oxygen or water vapour impurities on the silicon compact, and surface silica already present on the silicon particles will react with silicon to form silicon monoxide: silicon monoxide will also be formed by reactions involving water vapour, silicon and silica. Increasing the partial pressure of silicon monoxide in "static" experiments by increasing the amount of oxygen (up to 1×10^{-2}) or water vapour therefore increases the amount of α-silicon nitride. This mechanism is supported by the formation of silicon nitride with greater than 90% of the α-silicon nitride phase in fully reacted compacts of silicon and up to 2 wt % silica nitrided in "static" experiments [26].

Under "flow" conditions at an oxygen concentration of 5×10^{-6} the partial pressure of silicon monoxide at the sample surface will be reduced (compared to the equivalent "static" experiment) so reducing the quantity of α-silicon nitride formed (41% cf. 75%). At the same time the amount of silicon available for a direct reaction with nitrogen is increased leading to an increased amount of β-silicon nitride (formed below and/or above the melting point of silicon). Higher β-silicon nitride contents have also been observed for compacts prepared from this powder in "flow" experiments compared to "static" experiments when nitriding temperatures have been restricted to a maximum of 1350° C [27]. As the oxygen concentration of the nitriding gas increases (up to 1×10^{-2}) at constant flow rate, the partial pressure of silicon monoxide at the sample surface increases offsetting the reduction caused by gas flow, and the amount of α-silicon nitride therefore increases and the amount of β-silicon nitride decreases.

As the oxygen concentration increases beyond 1×10^{-2} for both "static" and "flow" experiments, the amount of α-silicon nitride decreases and there is a corresponding increase in the amount of β-silicon nitride. Under these conditions the silicon monoxide partial pressure probably begins to exceed the equilibrium partial pressure for the reaction $Si + SiO_2 = 2SiO$ and reaction rates are reduced due to the formation of protective silica layers. Therefore, an increased amount of the ceramic is formed during nitriding at 1450° C when it forms from liquid silicon as β-silicon nitride. Reductions in reaction rates due to silica formation at high oxygen concentrations are obviously more severe in a gas "flow" system than in a "static" system since in a "static" system very little nitriding gas (and its associated oxygen contamination) enters the furnace at low reaction rates. This explains why the β-silicon nitride content increases more rapidly in "flow" experiments than in "static" experiments. It also explains why cristobalite forms in "flow" experiments at an oxygen concentration of 5×10^{-2} but not in "static" experiments even at oxygen concentrations of 2×10^{-1}.

It should be noted that although there is an increased amount of silicon nitride formed from liquid silicon at oxygen concentrations in excess of 1×10^{-2} (excluding experiments where silicon oxynitride and silica are formed) these additional β-silicon nitride regions must be smaller than the strength controlling defects since they are formed under experimental conditions where strength is invariant with oxygen concentration (Fig. 6).

4.4. The composition of α-silicon nitride

The range of unit cell dimensions for the α-silicon nitride phase from this work agrees very closely with the literature values for samples prepared by the nitridation of silicon [13, 28–34]: this range is considerably smaller than for α-silicon nitrides prepared from silicon compounds [15, 17, 19, 35, 36] (Table IV). Unit cell dimensions have also been measured for α-silicon nitrides prepared from mixtures of silicon and silica [26]: the cell dimen-

sions were $[a] = 7.750 \pm 0.002$ Å and $[c] = 5.619 \pm 0.001$ Å. These narrow ranges in cell dimensions strongly suggest there cannot be large variations in the composition of the α-silicon nitrides prepared in this work despite the large amounts of oxygen or water vapour (or silica) in the nitriding reaction. The low oxygen content of samples with high proportions of α-silicon nitride confirms earlier data [15, 16, 18] that α-silicon nitride does not necessarily require the level of oxygen previously suggested for structural stability [13, 14].

4.5. X-ray profile shapes, "apparent" crystallite size and coefficient of variation in strength

It has been shown there are trends and relationships between the coefficient of variation in strength, water vapour concentration and X-ray profile shapes (Section 3.3). A rigorous analysis of profile shapes [37] was not attempted, but it is instructive to examine *Bw* in terms of the "apparent" crystallite size using the Scherrer formula [38], assuming a crystallite shape factor of unity. Fig. 7 shows a trend between "apparent" crystallite size and water vapour concentration: linear relationships between "apparent" crystallite size and coefficient of variation in strength ($r = -0.88$ for α_{540}) are shown in Fig. 8. A minimum coefficient of variation in strength (or strength variability) occurs at a water vapour concentration

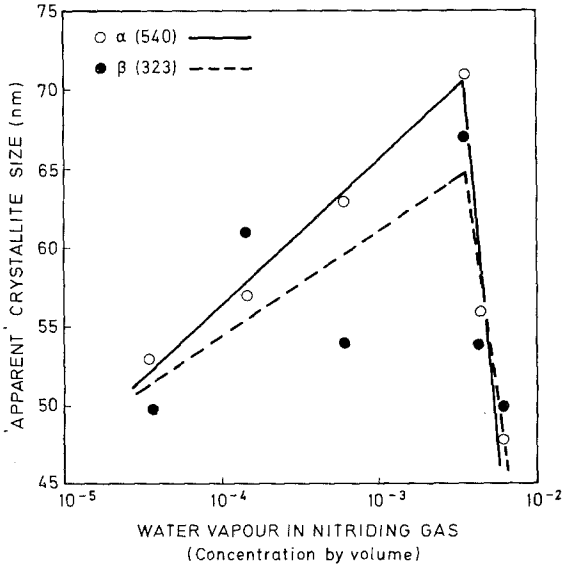

Figure 7 "Apparent" crystallite size versus concentration of water vapour in the nitriding gas for the α-nitride (5 4 0) peaks and β-nitride (3 2 3) peaks.

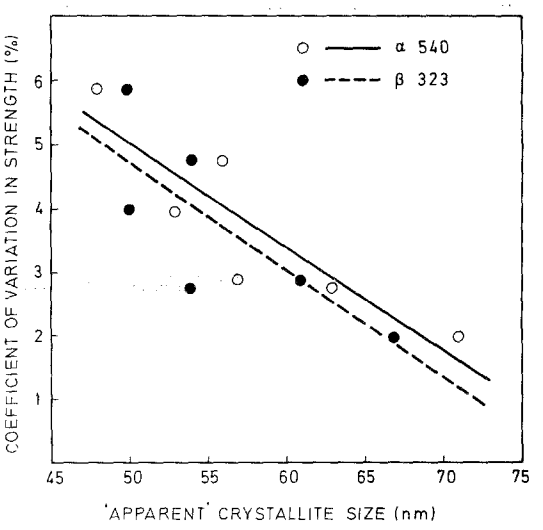

Figure 8 Coefficient of variation in strength versus "apparent" crystallite size for the α-nitride (5 4 0) peaks and the β-nitride (3 2 3) peaks. The straight lines are the least squares fit to the data.

$\sim 3.5 \times 10^{-3}$ corresponding to maxima in "apparent" crystallite sizes (~ 70 nm for α_{540}) and minima in *Bw*. A critical water vapour concentration (3.5×10^{-3}) probably influences nucleation, crystal growth and the "apparent" crystallite size in such a way that a uniform silicon nitride microstructure develops: this is reflected in the low coefficient of variation in strength. It is interesting to speculate whether other processing variables may reduce *Bw* and increase the "apparent" crystallite size, since low variability in strength is an important engineering requirement.

It is frequently stated that α-silicon nitride consists of a fine whisker matte, whilst β-silicon nitride is relatively coarser (e.g. [39, 40]). However, the similarity in "apparent" crystallite size for the two phases (Fig. 8) suggests that α- and β-silicon nitride form by similar mechanisms involving silicon monoxide and silicon vapour respectively: this does not exclude the formation of β-silicon nitride from liquid or solid silicon.

5. Conclusions

(1) High concentrations of oxygen or water vapour in the nitriding gas in "static" experiments have no significant effect on the strength of reaction sintered silicon nitride at room temperature and chemical contamination alone of the nitriding gas by these species is not responsible for abnormally low strength silicon nitride.

(2) The strength of reaction sintered silicon

nitride formed in "flow" experiments is approximately 30% lower than the strength in "static" experiments for corresponding oxygen concentrations up to 2×10^{-2}.

(3) Water vapour in the nitriding gas influences mechanical variability and X-ray profile shapes, and mechanical variability is related to the "apparent" crystallite size. A minimum in mechanical variability corresponds to a minimum X-ray line width and a maximum "apparent" crystallite size and occurs at a water vapour concentration of 3.5×10^{-3}.

(4) The "apparent" crystallite size for α- and β-silicon nitride are similar.

(5) The amount of α-silicon nitride increases as the oxygen and water vapour in the nitriding gas increase, suggesting that α-silicon nitride may be formed by reactions involving monoxide and nitrogen.

(6) The higher β-silicon nitride contents for samples prepared under "flow" at low oxygen concentrations are probably a consequence of an increase in the contribution of a direct silicon/nitrogen reaction which may involve silicon in the vapour phase.

(7) The low variability in lattice parameters indicates there cannot be a large variation in the composition of α-silicon nitride in our samples. The low measured oxygen contents for high α-silicon nitride samples confirms earlier data that α-silicon nitride does not necessarily require the previously suggested amount of oxygen for structural stability.

Acknowledgements

The authors acknowledge the experimental assistance of Miss A. J. Edwards, K. C. Pitman and W. May and many helpful discussions with Dr B. F. Jones. This paper is published with the permission of the Ministry of Defence (Procurement Executive): and of the Controller HMSO, holder of Crown Copyright.

References

1. D. J. GODFREY, *Proc. Brit. Ceram. Soc.* **22** (1973) 1.
2. B. F. JONES and M. W. LINDLEY, *J. Mater. Sci.* **10** (1975) 967.
3. *Idem, ibid* **11** (1976) 191.
4. D. J. GODFREY and M. W. LINDLEY, *Proc. Brit. Ceram. Soc.* **22** (1973) 229.
5. D. R. MESSIER and P. WONG, *J. Amer. Ceram. Soc.* **56** (1973) 480.
6. K. J. HÜTTINGER, *High Temp. – High Pressures* **1** (1969) 221.
7. D. R. MESSIER, P. WONG and A. E. INGRAM, *J. Amer. Ceram. Soc.* **56** (1973) 171.
8. R. B. GUTHRIE and F. L. RILEY, *Proc. Brit. Ceram. Soc.* **22** (1973) 275.
9. K. J. HÜTTINGER, *High Temp. – High Pressures* **2** (1970) 89.
10. R. G. FRIESER, *J. Electrochem. Soc.* **115** (1968) 1092.
11. K. BLEGEN, "Special Ceramics 6", edited by P. Popper (British Ceramic Research Association, Stoke-on-Trent, 1975) p. 223.
12. R. B. GUTHRIE and F. L. RILEY, *J. Mater. Sci.* **9** (1974) 1363.
13. S. WILD, P. GRIEVESON and K. H. JACK, "Special Ceramics 5", edited by P. Popper (British Ceramic Research Association, Stoke-on-Trent, 1972) p. 385.
14. I. COLQUHOUN, S. WILD, P. GRIEVESON and K. H. JACK, *Proc. Brit. Ceram. Soc.* **22** (1973) 207.
15. H. F. PRIEST, F. C. BURNS, G. L. PRIEST and E. C. SKAAR, *J. Amer. Ceram. Soc.* **56** (1973) 395.
16. A. J. EDWARDS, D. P. ELIAS, M. W. LINDLEY, A. ATKINSON and A. J. MOULSON, *J. Mater. Sci.* **9** (1974) 516.
17. I. KOHATSU and J. W. McCAULEY, *Mater. Res. Bull.* **9** (1974) 917.
18. K. KIJIMA, K. KATO, Z. INOUE and H. TANAKA, *J. Mater. Sci.* **10** (1975) 362.
19. K. KATO, Z. INOUE, K. KIJIMA, I. KAWADA, H. TANAKA and T. YAMANE, *J. Amer. Ceram. Soc.* **58** (1975) 90.
20. K. LIDELL and D. P. THOMPSON, private communication (to be published).
21. C. P. GAZZARA and D. R. MESSIER, AMMRC-TR75-4, US Army Materials and Mechanics Research Centre, Watertown, Mass, February 1975.
22. G. ASTLE and I. F. FERGUSON, "Firestar and Firecracker", UKAEA Report TRG 1812 (S) (1970).
23. B. F. JONES and M. W. LINDLEY, *J. Mater. Sci.* **11** (1976) 1288.
24. K. C. PITMAN, unpublished data.
25. A. HENDRY and K. H. JACK, "Special Ceramics 6", edited by P. Popper (British Ceramic Research Association, Stoke-on-Trent, 1975) p. 199.
26. D. P. ELIAS and M. W. LINDLEY, unpublished data.
27. D. P. ELIAS, B. F. JONES and M. W. LINDLEY, *Powder Met. Int.*, to be published.
28. D. HARDIE and K. H. JACK, *Nature* 180 (1957) 332.
29. S. N. RUDDLESDEN and P. POPPER, *Acta Cryst.* **11** (1958) 465.
30. W. D. FORGENG and B. F. DECKER, *Trans. Met. Soc. AIME* **212** (1958) 343.
31. H. J. GOLDSCHMIDT and J. A. BRAND (1959) private communication.
32. H. SUZUKI, *Bull. Tokyo Inst. Tech.* **54** (1963) 163.
33. D. S. THOMPSON and P. L. PRATT, *Science of Ceramics* **3** (1967) 33.
34. C. M. B. HENDERSON and D. TAYLOR, *Trans. Brit. Ceram. Soc.* **74** (1975) 49.

35. R. MARCHAND, Y. LAURENT, J. LANG and M. Th. Le BIHAN, *Acta Cryst.* **B25** (1969) 2157.
36. F. GALASSO, U. KUNTZ and W. J. CROFT, *J. Amer. Ceram. Soc.* **55** (1972) 431.
37. D. LEWIS and M. W. LINDLEY, *J. Amer. Ceram. Soc.* **47** (1964) 652.
38. P. SCHERRER, *Gottinger Nachrichten* **2** (1918) 98.
39. A. DE S. JAYATILAKA, T. F. PAGE and J. A. LEAKE, *J. Mater. Sci.* **9** (1974) 514.
40. N. L. PARR, G. F. MARTIN and E. R. W. MAY, "Special Ceramics", edited by P. Popper (Academic Press, for British Ceramics Research Association, 1960) p. 102.

Received 21 November 1975 and accepted 9 February 1976.